Electrochimica Acta 54 (2009) 2342–2352

Contents lists available at ScienceDirect

Electrochimica Acta

journal homepage: www.elsevier.com/locate/electacta

Perfluorinated nanocomposite membranes modified by polyaniline: Electrotransport phenomena and morphology

N.P. Berezina [a,*], N.A. Kononenko [a], A.A.-R. Sytcheva [b], N.V. Loza [a], S.A. Shkirskaya [a], N. Hegman [b], A. Pungor [b]

[a] Department of Physical Chemistry, Kuban State University, 149, Stavropolskaya St., Krasnodar 350040, Russia
[b] Department of Nanometrology, Bay Zoltan Institute for Nanotechnology, Miskolc-Egyetemváros 3515, Hungary

ARTICLE INFO

Article history:
Received 16 July 2008
Received in revised form 26 October 2008
Accepted 28 October 2008
Available online 5 November 2008

Keywords:
Perfluorinated ion-exchange membrane
Polyaniline
Conductivity
Diffusion permeability
Water transport
Polarization phenomena

ABSTRACT

This work summarizes results on the modification of perfluorinated sulfocationic membranes MF-4SC by in situ chemical polymerization of aniline. The investigation of transport properties of polyaniline/MF-4SC composite membranes after bulk modification – conductivity, diffusion and electroosmotic permeability, proton permselectivity – as well as porosimetry and polarization behavior is carried out as functions of aniline polymerization parameters and acid concentration. The fibrous-cluster model of a composite membrane is proposed for the estimation of transport and structural parameters, taking into account different mechanism of charge transfer in structural fragments of the composite. The atomic force microscopy images and curves of water distribution on the effective pore radii in the composite membranes testify to a morphological transition from the nano- to the microsize of polyaniline inclusions with increasing the aniline polymerization time. This effect is confirmed by the analysis of two-phase model transport and structural parameters. High values of the "true" proton transport numbers of composites are obtained and discussed. The dynamic hydration numbers of protons and chloride co-ions are estimated using the "true" transport numbers of protons and the electroosmotic coefficients of composites. The current–voltage curves of composite membranes in the "free standing" state after bulk and surface modification by polyaniline are investigated. The effect of stabilization of limiting current density is observed for MF-4SC membrane after bulk modification. The effect of current–voltage curves asymmetry is observed for different orientation of the polyaniline layer towards the current direction for an anisotropic composite membrane after surface modification.

1. Introduction

The synthesis of composite ion-exchange materials and investigation of their functional properties are relatively new research area in membrane electrochemistry and high-molecular chemistry. Lately, this area has attracted the interest of researches, which is due to the development of fuel cells and various sensor devices. Also, there are a number of electrochemical processes done on the industrial scale, which need advanced materials for the construction not only of electrodes but and separation diaphragms. Such composites are applied as separation membranes in electrodialysis, as solid electrolyte with high proton conductivity in the membrane–electrode modules of fuel cells, in polymer microelectronics and biosensors [1–10]. The two main functions of polymer composite materials in fuel cells and other electrochemical reactors are as follows: first, they provide high proton conductivity between the cathode and the anode; second, they separate the cathode and anode spaces and, in this way, suppress chemical interaction between the fuel and the oxidant [11–14]. Perfluorinated sulfocationic membranes of type Nafion® (Du Pont, USA) [15] and MF-4SC (Plastpolymer, Russia) [16] possess special properties, such as high thermal and chemical stability along with good conductivity. These membranes are used as a template for the synthesis of various composites. Recently, research has been focused on Nafion® membranes modified by conducting polymers, such as polyaniline that exhibits unique electrical, electrochemical and optical properties [1,2,17–20].

The investigation of composites in a "free standing" state based on perfluorinated sulfocationic membranes and polyaniline is of special interest because such composite materials can be used to promote the efficiency of electromembrane separation processes [21–23]. Most often such materials are obtained by chemical template synthesis, where various redox systems are electron acceptors during the oxidative polymerization of aniline [24–26].

* Corresponding author. Tel.: +7 861 219 95 73; fax: +7 861 219 95 73.
E-mail address: ninel_berezina@mail.ru (N.P. Berezina).

0013-4686/$ – see front matter © 2008 Elsevier Ltd. All rights reserved.
doi:10.1016/j.electacta.2008.10.048

The aim of this work is to summarize the results of investigation of composites based on perfluorinated sulfocationic membranes MF-4SC and polyaniline (the latter is introduced into the original matrix by chemical synthesis) [27–30]. One of the tasks of this work is to establish a correlation between the structural characteristics and transport properties of the composites and to obtain composite materials with a set of optimal characteristics. The development of theoretical approach to the description of macroscopic transport phenomena in the composite membranes is an actual problem in modern electrochemistry and materials science presented in this article.

2. Experimental

2.1. Materials

A Nafion type perfluorinated sulfocationic membrane (MF-4SC) produced by "Plastpolymer" (St.-Petersburg, Russia) was used as a template matrix for composite membranes preparation. These composite membranes were obtained by the penetration of polyaniline (PAni) into the initial (non-modified) membrane. The oxidative–thermal conditioning technique of perfluorinated membranes includes sequential boiling of the MF-4SC membranes in 5% HNO_3, 10% H_2O_2 aqueous solutions and distilled water for 3 h in each case [31].

It is known that membranes Nafion and MF-4SC have so-called cluster morphology. Their amorphous zone is characterized by a number of nanosized structural elements: from narrow channels of 1.5 nm in diameter up to ion-cluster zones ("pores") of 5–6 nm in diameter. The size of crystallites introduced into the amorphous zone is up to 20 nm [32]. The polymer matrix of a perfluorinated membrane is sort of a nanoreactor for aniline polymerization, because the formation of PAni chains occurs in the restricted nanospace of structural cavities of the matrix. The template synthesis of PAni allows to obtain particularly nanostructured polymer material.

A template synthesis of polyaniline in the MF-4SC matrix was performed by a chemical method described elsewhere [28,30,33]. A membrane fixed in a vertical position was located between solutions of 0.01 M $FeCl_3$ in 0.5 M H_2SO_4 (oxidant), and 0.01 M aniline in 0.5 M H_2SO_4. The polymerization was carried out in a two-chamber cell using a counter diffusion method. After a time period which depends on the sample pretreatment, the membrane turns blue and then, rapidly, emerald-green. As a result, composite membranes (PAni/MF-4SC) with different color intensity could be prepared varying the time of in situ oxidation of aniline. An emerald-green membrane (5 h of synthesis) and a black one (30 days of synthesis with regular change of polymerization solutions) were investigated in this work. The color intensity depends on the ratio between oxidized (doped) and reduced (undoped) forms of polyaniline, i.e. on the exposure time in working solutions [34]. Chemical forms of polyaniline are described in details elsewhere [1,24,35].

Physical and chemical characteristics of the investigated samples are shown in Table 1.

One can see that the weight fraction of PAni (in the swollen state of the membrane) increases from 12.4% to 17.2% despite the time of synthesis has increased significantly. In our opinion, after 30 days of synthesis the membrane is fully saturated with PAni. Before measurements, the obtained composite membranes were held in acid solutions of a certain concentration.

2.2. Membrane characterization

2.2.1. Equilibrium properties

Several standard techniques have been used to test the membranes [36]. The ion-exchange capacity Q was determined for H^+-form samples by "shifting the equilibrium with titrant excess". The samples were kept in a 5% KCl solution in 0.1 M KOH for 24 h. After the ion-exchange was completed, the excess of KOH was titrated by a 0.1 M HCl solution in the presence of a mixed indicator and the content of $-SO_3H$ groups in the swollen sample was calculated.

The water uptake of membranes MF-4SC was measured by drying H^+-form samples in the air. The water was evaporated at 105 °C, and the value of water fraction was obtained as the ratio between the weight loss and the weight of the wet membrane sample. The membrane hydration capacity n_m (average number of H_2O moles per 1 mol of functional groups) was calculated from the values of water content and ion-exchange capacity of the samples; the accuracy of determination of n_m was as low as 0.1 mol H_2O/mol $-SO_3^-$ [37]. The characteristics obtained are shown in Table 1.

The method of standard contact porosimetry was used for the determination of water distribution in membrane "pores" [38–42]. In the standard porosimetry method, the water content is measured for the membranes equilibrated with standards of a definite porous structure. For the standards, the integral curves of distribution of pore volume on the effective pore radii were obtained by independent techniques, such as capillary condensation. The "resolution" of standard porosimetry is about 1 nm (that is, an average molecule size of the liquids used in this research).

2.2.2. Microscopy measurements

Atomic force microscopy (AFM) [43,44] images were recorded in the tapping mode using a NTEGRA Spectra AFM instrument (NT-MDT, Russia) with high-resolution non-contact silicon gold-coated tips. Before the measurements, the membranes were conditioned in a 0.5 M H_2SO_4 solution with subsequent rinsing in distilled water and drying for at least 24 h at a temperature of 105 °C. This method was successfully applied for the investigation of the surface of Nafion-117 [45,46] membranes after saturating them with organic components.

The morphology and microstructure of anisotropic composite membranes were characterized using scanning electron microscopy (SEM) (Hitachi S-4800, Japan) [47,48]. SEM samples were dried and sputtered with gold to reduce charging effects during measurements. Elemental analysis of the membranes was performed using energy-dispersive X-ray spectroscopy (EDS) method (Quantax system, Bruker AXS, Germany).

2.2.3. Transport properties

The membrane conductivity κ_m (S/m) was determined from the value of membrane resistance measured as the real part of

Table 1
Physicochemical properties of perfluorinated sulfocationic membranes MF-4SC with and without polyaniline.

Membrane	Thickness (l) (cm)	Saturation degree, g PAni/g wet membrane (%)	Water uptake, g H_2O/g wet membrane (%)	Ion-exchange capacity (Q), mmol H^+/g wet membrane	Hydration capacity (n_m), mol H_2O/mol $-SO_3^-$
MF-4SC	0.027–0.028	–	25.2	0.86	16.3
PAni/MF-4SC (5 h of synthesis)	0.028–0.029	12.4	21.9	0.93	13.1
PAni/MF-4SC (30 days of synthesis)	0.030–0.031	17.2	20.1	1.11	10.0

membrane impedance [42,49]. We used mercury electrodes operating at 50–500 kHz AC with a TESLA BM-507 impedance-meter. The mercury contact method is widely used for studying polymer films since this technique provides an ideal contact between the electrodes and the sample. Moreover, this method is not limited by the concentration of the equilibrium solution or by water content in the membrane, which may vary for different polymer materials.

Polarization effects in membranes lead to discrepancies between the conductivity of an ion-exchange membrane measured under alternating current (κ_{AC}) and that measured under direct current (κ_{DC}). A simple equation establishing the relationship between these characteristics has been derived and confirmed by experimental data for heterogeneous electrodialytic membranes [42]:

$$\kappa_{DC} = \kappa_{AC} \cdot t_i^{f_2} \quad (1)$$

where t_i is transport number of counter-ions in solution; f_2 is the volume fraction of equilibrium solution in the membrane. For homogeneous membranes, when $f_2 \to 0$, the discrepancies between κ_{AC} and κ_{DC} can be neglected. Processing the concentration dependence of membrane conductivity in H_2SO_4 solutions within the frames of the two-phase conductivity model allows to calculate both the volume fraction of free solution inside the membrane phase (f_2) and the value of conductivity at the isoconductivity point (κ_{iso}) [42,50,51].

The diffusion of electrolyte through a membrane is described by several quantitative parameters: the electrolyte diffusion flux (j_m, mol/m^{2}s), the integral (P_m, m^2/s) and differential (P^*) coefficients of diffusion permeability. The relationships between these parameters are defined by the following equations:

$$j_m = \frac{V}{S} \cdot \frac{dc}{d\tau} \quad (2)$$

$$j_m = -P^* \frac{dc}{dl} \quad (3)$$

$$P_m = \frac{\int_0^c P^* dc}{c} \quad (4)$$

$$P^* = \frac{d \ln j_m}{d \ln c} \cdot \frac{j_m \cdot l}{c_0} = \beta \frac{j_m \cdot l}{c_0} \quad (5)$$

where S is the membrane area, $dc/d\tau$ is the rate of electrolyte accumulation in a compartment of volume V initially filled with water (in diffusion cell), parameter β, which characterizes the shape of the concentration profile in a membrane, is obtained from double logarithmic j–c plots, l is the membrane thickness, while c and c_0 are the solution concentrations at time τ and an initial instant, τ_0, respectively. We studied the diffusion of a H_2SO_4 acid solution through a membrane to pure water [36,42]. The rate of increase of the acid concentration in the chamber filled with water ($dc/d\tau$) was controlled by conductometry.

The electrotransport characteristics of membranes were determined in a wide concentration range of H_2SO_4. The experimental data on the conductivity and diffusion permeability of initial and composite membranes were used to calculate ion transport numbers applying the procedures described elsewhere [29,42]. These experimental data were also used for the calculation of transport and structural parameters (TSPs) of membranes by applying a model approach and computer simulations [42,52–54].

Electroosmotic permeability of the membranes in HCl solutions was defined as the water transport number t_w (mol H_2O/F) and was measured in a two-chamber cell with reversible silver chloride electrodes by the volumetric method [36,42,55,56]. The values of t_w were calculated from the following relationship:

$$t_w = \frac{V^* \cdot F}{v_m S \cdot i \cdot \tau} \quad (6)$$

where V^* is the volume of water transferred, i is current density, τ is time period, v_m is mole water volume (18 cm^3/mol), F is the Faraday number, S is the effective membrane surface area.

2.2.4. Membrane voltammetry

The membrane voltammetry method is capable of measuring polarization properties of membranes under conditions approximating those of actual membrane operation. Each portion of a current–voltage curve (CVC) provides information about electrotransport properties of the membrane. The ohmic portion helps determine the membrane resistance. The value of limiting electrodiffusion current (i_{lim}, A/m^2) depends on the membrane permselectivity, concentration and chemistry of the electrolyte solution as well as on hydrodynamic conditions, which influence the thickness of diffusion layer on the membrane surface. Backward diffusion of the electrolyte solution can increase the i_{lim} value in accordance with the following equation [57]:

$$i_{\lim} = \frac{D \cdot c \cdot F}{(t_i^* - t_i)\delta} + \frac{P^* \cdot c \cdot F}{(t_i^* - t_i)l} \quad (7)$$

where D is the electrolyte diffusion coefficient in solution, δ is the thickness of diffusion layer, c is the concentration of solution, t_i and t_i^* are transport numbers of counter-ions in solution and membrane, respectively.

The increase of the current above i_{lim} is caused by the coupled effects of concentration polarization inducing electro-, thermo- and gravitational convective flows. These effects are the generation of H^+, OH^--ions and the formation of macroscopic spatial charge in solution at the membrane/solution interface, and the limiting current exaltation [51,58–63]. Hydrodynamic and structural features of the membrane surface determine the behavior of the membrane under overlimiting currents.

The distinguishing parameters of CVCs to be used for testing the membrane materials are as follows: the slope of the ohmic portion, the limiting current value, the length of limiting current plateau (Δ, V), and the potentials, where transitions to the limiting (ΔE_{lim}, V) and overlimiting (ΔE_{cr}, V) states occur. The CVCs of membrane composites PAni/MF-4SC were obtained in the galvanodynamic regime in a cell equipped with platinum polarizing and silver chloride measuring electrodes (Fig. 1) [64]. The hydrodynamic regime used in this work is characterized by Reynolds numbers from 6 to 4. This implies that measurements of CVCs for ion-exchange membranes occur under conditions of the laminar flow of solution. The value of the electrodiffusion limiting current density i_{lim} was found graphically from the voltammetry curves with the aid of the program Microsoft Excel.

The experiments were carried out at a temperature of 25 °C. The measurement errors for all determined parameters were in the range of 3–5%.

3. Results and discussion

3.1. Transport and structural parameters of original and composite membranes

3.1.1. Model approach to membrane characterization

In a number of works we described an approach to the characterization of ion-exchange membranes, which is based on the model of structural and electrochemical inhomogeneity of the material. When the membrane is modified, its structure becomes more complex due to the appearance of a new structural element, polyaniline, which has the polaron mechanism of charge transfer in the doped state [1]. At present, there is no model approach in literature to the description of transport properties of membrane composites based

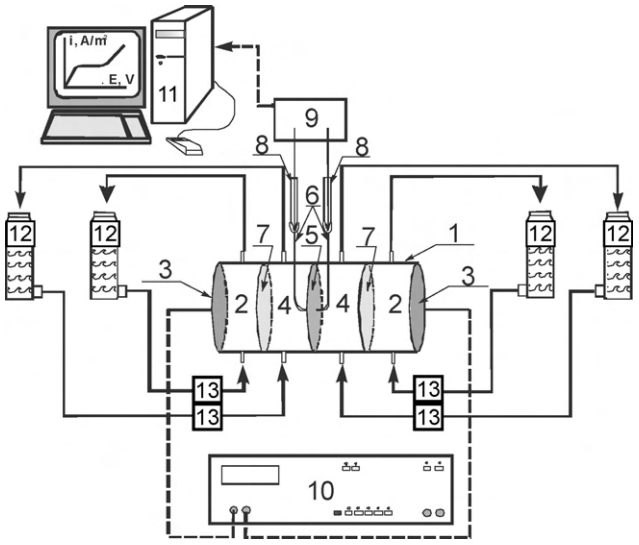

Fig. 1. Schematic view of setup for current–voltage curve measurements: (1) measuring cell; (2) near-electrode compartments; (3) platinum polarizing electrodes; (4) near-membrane compartments; (5) membrane under investigation; (6) probes; (7) auxiliary membranes; (8) silver chloride electrodes; (9) pH-meter-ion meter "Expert-001"; (10) potentiostat PI-50-1.1; (11) computer; (12) solution vessels; (13) multichannel peristaltic pump "Zalimp pp. 1–05". The hydrodynamic scheme is in solid lines, while the electric circuit is in dashed lines.

on electroactive polymers. In this work, an emphasis is made on the characterization of composite membranes of type "polymer in polymer" from the viewpoint of a modified two-phase model of the membrane material structure.

The well-known Nernst–Planck equation

$$j_i = -L_i^* \, grad \, \mu_i^* \tag{8}$$

can be used as a differential transport equation for *i*-type ions that move under electrochemical potential gradient ($grad\,\mu_i^*$). j_i characterizes the ion flux and L_i^* is the coefficient of proportionality between the ion flux and the force acting on the ion. Phenomenological coefficients L_i^* are electrodiffusion characteristics of the ion mobility in a heterogeneous medium. It has been suggested [65] that these factors are functions of conducting properties of membrane "pseudo-phases" and of membrane geometry (packing factors of conducting phases). The theory of generalized conductivity for a heterogeneous system [51,42,65] provides a basis for quantitative characterization of electrochemical properties of membranes. The effective properties are defined as characteristics of separated phases by the interpolating equation proposed independently by K. Lichtenecker and N.P. Gnusin:

$$L_m^* = [f_1 L_1^\alpha + f_2 L_2^\alpha]^{1/\alpha} \tag{9}$$

In this equation L_m is the coefficient of generalized conductivity (conductivity or diffusion permeability coefficient); L_1, L_2 are properties of individual phases; f_1 and f_2 are the volume fractions of phases; α is a parameter characterizing the space orientation of phases in the material. Parameters f and α are related to the geometry of dispersion.In the case of 1:1 electrolyte (such as NaCl), the resulting membrane conductivity and diffusion permeability coefficient can be expressed as follows:

$$\kappa_m = [f_1 \kappa_{iso}^\alpha + f_2 \kappa^\alpha]^{1/\alpha} \tag{10}$$

$$P^* = [f_1 (Gc)^\alpha + f_2 D^\alpha]^{1/\alpha} \tag{11}$$

Here κ_{iso} and κ are specific conductivities of phase I and of solution, respectively; c is solution concentration; D is the electrolyte diffusion coefficient in solution. G is a complex parameter [42] which contains the Donnan constant (k_D), the co-ion diffusion coefficient in phase I ($\bar{D}_-$) and the membrane exchange capacity:

$$G = \frac{k_D \cdot \overline{D_-}}{Q} \tag{12}$$

Parameter G plays the same role in diffusion as parameter κ_{iso} does in conductivity. κ_{iso} is a characteristic of the counter-ions transport and G is that of the co-ions transport in phase I.

The proposed model of a composite membrane PAni/MF-4SC preserves the selection of two conducting "pseudophases". We use the term "pseudophase" in this model because all structural fragments have no visible phase boundaries. A simplified model of the composite membrane is shown in Fig. 2. Pseudophase I is considered to consist of ion-cluster zones of the base membrane with either ion or proton (in acid solutions) conductance and of polyaniline aromatic chains. The contribution of the polaron conductance of polyaniline depends on the degree of doping of quinone-imine fragments [1]. All non-conductive fragments (fluoroethylene chains, microcrystallites and uncharged PAni units) are included in pseudophase I of a volume fraction of f_1. The second pseudophase includes either inner electrolyte solution or water being dispersed in the bulk of the composite, outside the electric field of charges on polymer chains. It is supposed that the inner electrolyte solution has the same characteristics as the outer equilibrium solution. The volume fraction of the inner solution is f_2, while $f_1 + f_2 = 1$. In Fig. 2 different cases of conducting phase orientation are presented: $\alpha \to +1$ for parallel orientation, $\alpha \to -1$

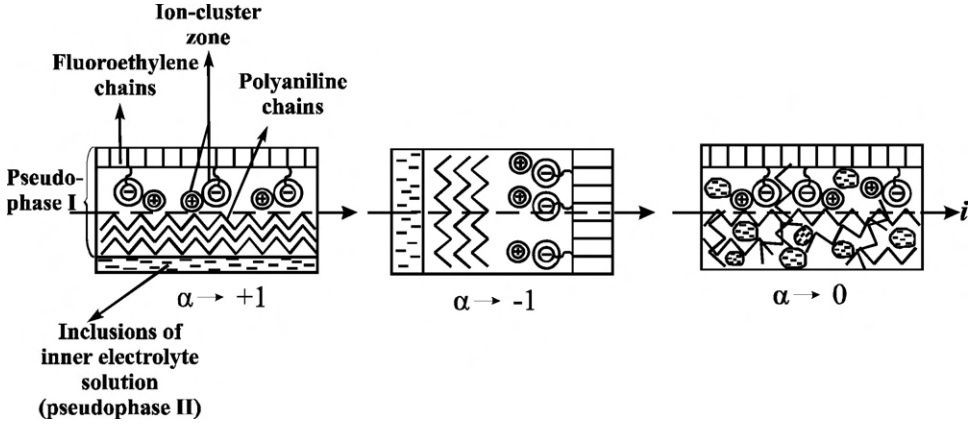

Fig. 2. Simplified two-phase model of a membrane MF-4SC incorporating polyaniline and schematic presentation of "pseudophases" space orientation towards the current direction: (1) fluoroethylene chains; (2) ion-cluster zone; (3) polyaniline chains; (4) inclusions of inner electrolyte solution.

Table 2
Transport and structural parameters of membranes in a H_2SO_4 solution.

Membrane	f_2	κ_{iso} (S/m)	α	$G \times 10^{16}$ m^5/(mol s)
MF-4SC	0.06	4.23	0.30	156.3
PAni/MF-4SC (5 h of synthesis)	0.08	4.38	0.27	107.5
PAni/MF-4SC (30 days of synthesis)	0.16	1.14	0.10	2.2

for serial orientation and $\alpha \to 0$ for random phase distribution, respectively.

Taking into account the fact that under certain conditions PAni forms nanosized fibrils [25,66–68], let us call the model in question as a fibrous-cluster one. This model is simplified because it does not consider chemical and cooperative interactions between the structural fragments. Parameters $\alpha, f_2, \kappa_{iso}, G$ for a composite membrane are calculated by the same equations as for the base membrane without modifying component [42,52–54]. In works [42,52] we suggested to supplement this set of TSPs by the dynamic hydration numbers of counter- and co-ions in the membrane, h^*_+ and h^*_-. In order to calculate these characteristics, the measurement of membrane electroosmotic permeability and "true", or electromigration, counter-ion transport numbers as functions of solution concentration is required.

3.1.2. Transport properties: conductivity and diffusion permeability

Concentration dependences of conductivity and diffusion flux of base and composite membranes in H_2SO_4 solutions are shown in Fig. 3a and b. In order to characterize the membranes more fully, these results are complemented by calculated dependences of "true" proton transport numbers through the membranes (Fig. 3c) and experimental dependences of water transport numbers in HCl solutions (Fig. 3d).

From Fig. 3, it can be seen that the conductivity and diffusion flux of the composite membrane after 5 h of synthesis (weight fraction of PAni is 12.4%) are practically the same as of the base MF-4SC membrane. TSPs calculated on the basis of these data are given in Table 2, where of it can be concluded that the set of TSPs ($\alpha, f_2, \kappa_{iso}$) does not change substantially. An exception is parameter G, which decreases by 1.45 times [29]. Polyaniline in the membrane exists in the form of emeraldine (the color of samples is green), which is confirmed by spectroscopic measurements in the UV–vis range in paper [28]. Despite there is no synergetic effect of increase of the composite conductivity, the electron conductivity of emeraldine compensates for the decrease of proton conductivity, which is due to the appearance of phenylammonium ions during the template synthesis [30]. Such behavior of the composite can be explained by the nanometric size of emeraldine inclusions.

For the membrane after 30 days of synthesis being saturated with PAni (its weight fraction is 17.2%) a decrease of conductivity and diffusion flux by 3–4 times in the whole range of acid concentration is observed (Fig. 3a and b, curve 3). The calculation of TSPs has shown a two-fold increase of parameter f_2 and a three-fold decrease of parameter α (Table 2). Within this model such a change of these parameters indicates the increase of number of structural cavities filled with solution (increase of parameter f_2) and the orientation of pseudophases becomes more chaotic, i.e. dispersity of the system increases (Fig. 2). Due to the fact that PAni fibrils can ramify during growth [69], being penetrated into amorphous, cluster zones, they block transport paths for ion transfer through pseudophase I. In fact, parameter κ_{iso} characterizing the proton conductivity in pseudophase I decreases by 3.5 times. The drop of parameter G is much more significant: it decreases by 72 times compared to the base membrane and by 50 times compared to the composite membrane in the emeraldine form. The effect of strong deceleration of co-ions is due to the influence of rigid aromatic PAni chains and their more chaotic orientation.

3.1.3. Permselectivity

The results of calculation of electromigration or "true" transport numbers [51,70], which characterize portion of current transferred by protons without hydration shell, are shown in Fig. 3c for all the membranes investigated. These dependences were calculated from the data on conductivity and diffusion permeability according to the equations shown in Fig. 3. In these equations, L_+ and L_- are electrodiffusion coefficients of counter- and co-ions, respectively; they are dependent upon the concentration of the equilibrium solution [71,72]. The non-ideality of the solution is taken into account by a parameter $\pi_\pm$ calculated by the following equation:

$$\pi_\pm(c) = 1 + \frac{d \ln \gamma_\pm}{d \ln c} \tag{13}$$

It can be seen from Fig. 3c that the composite membranes are highly selective to protons (curves 2 and 3). This is an unusual effect because "loosening" of the structure of MF-4SC membrane after 30 days of PAni synthesis and blocking of transport paths by polyaniline segments would lead to a decrease of selectivity. A reason for high selectivity of the composite membranes is compacting of the membrane cluster zones, which is due to "cross-linking" of the perfluorinated matrix by PAni chains, and decrease of the diffusion coefficient of acid anions in pseudophase I. It is a morphological effect which leads to the decrease of co-ions transport.

Another explanation for high selectivity of polymers containing imine groups was given by Riande and co-workers [73]. They assumed that a positive charge on the nitrogen atom of an imine group causes electrostatic interaction with co-ions. This leads to a decrease of the portion of current transferred by co-ions, while the portion of current transferred by protons increases. This effect may occur in the case of polyaniline containing composites as well [74]. Interaction of acid anions with positively charged imine groups leads to a decrease of co-ions contribution to the current transport. It is an electrostatic effect due to the ion pair formation in pseudophase I. Therefore, these effects are responsible for high proton permselectivity of both emeraldine and pernigraniline (dark-green or black color) composite membranes.

3.1.4. Electroosmotic permeability and dynamic hydration numbers

The dependences of calculated "true" proton transport numbers upon concentration are complemented by independent measurements of electroosmotic permeability in HCl solutions. It can be seen from Fig. 3d that transport numbers of water with proton are weakly dependent upon the acid concentration and time of polymerization of aniline in the membrane. The mechanism of water transport in the composites is discussed in paper [75].

The data on H^+ transport numbers were used for the estimation of dynamic hydration numbers of ions in the membranes. As it is shown in works [42,52], the equation presented in Fig. 3 is used for this purpose after modification taking into account that $t_+ + t_- = 1$:

$$t_w = t_+(h^*_+ + h^*_-) - h^*_-, \tag{14}$$

where t_+ is "true" transport number of counter-ion, h^*_+, h^*_- are dynamic hydration numbers of counter- and co-ions, respectively. The latter parameters are not related to the two-phase model; their physical sense is effective hydration characteristics of ions in the membrane as a whole.

As it follows from Eq. (14), the concentration dependences shown in Fig. 3c and d can be used for graphic determination of dynamic hydration numbers of both counter- and co-ions. It can be

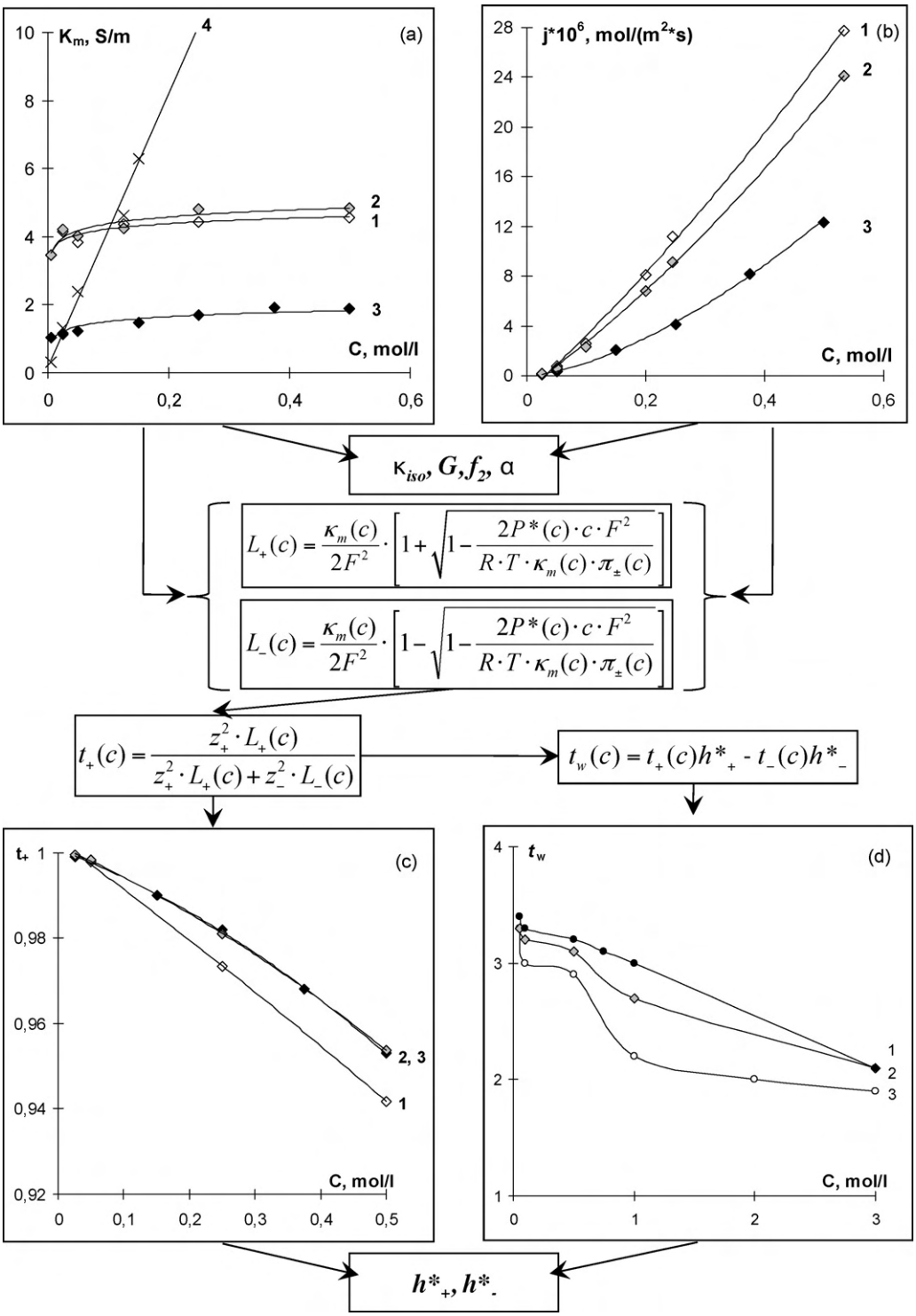

Fig. 3. Concentration dependences in acid solutions of conductivity (a), diffusion flux (b), "true" proton transport numbers (c) and water transport numbers (d) of a MF-4SC membrane (1), composites PAni/MF-4SC after 5 h (2) and 30 days (3) of aniline polymerization, and calculation equations.

seen from Table 3 that the values of h^*_+ for protons are in the range of 3.3–4, which is close to the experimental values of t_w. However, the hydration numbers of Cl^- anions h^*_- decrease significantly with increase of the aniline polymerization time. In an electric field, Cl^- co-ions transport the water molecules being closest to themselves (1–2 mol) [76,77] and involve in movement an additional volume of water. In composite membranes the diameter of transport channels decreases due to PAni inclusions. These morphological changes of the composite lead to distortion of the "dynamic" hydration shell of ions. The decrease in the transport number of water together with Cl^- ion is in agreement with the decrease of its kinetic characteristics, such as diffusion coefficient and ion transport number. At the same time, proton, which transports water in the form of strong hydroxonium complexes [75,78] and is capable of transport by the relay mechanism, retains practically constant values of effective dynamic hydration numbers.

Table 3
Dynamic hydration numbers of ions in ion-exchange membranes.

Membrane	h^*_+	h^*_-
MF-4SC	3.3	11.4
PAni/MF-4SC (5 h of synthesis)	3.3	8.8
PAni/MF-4SC (30 days of synthesis)	4.0	4.3

Therefore, the analysis of TSPs showed that the evolution of PAni oxidation state and its morphology in the perfluorinated membrane leads to the compacting of pseudophase I and to decrease of its volume fraction f_1 at the expense of the volume fraction of inner solution f_2 ($f_1 + f_2 = 1$). This process is accompanied by changing of space orientation of conducting phases (Fig. 2). Based on the analysis of TSPs, it is possible to conclude that the nanometric size of PAni inclusions in particular makes the composite membrane after 5 h of synthesis retain its conductive properties. The absence of synergetic effect in the membrane overall conductivity indicates that PAni does not form a percolation path for electron conductance in the membrane [30]. The increase of PAni content in the membrane and of its oxidation degree (in the case of PAni/MF-4SC after 30 days of synthesis) leads to re-organization of the structure of transport channels. This is accompanied by a transition from nanosized to microsized PAni inclusions, which results in a change of all TSPs and is confirmed by independent measurements of the composite morphology.

3.2. Structure of composites investigated by AFM and standard porosimetry methods

The advantage of AFM over SEM is that AFM can probe the surface of the membrane without using a radiation source, which can burn the surface, and without adding a gold layer, which could slightly alter the topography of the membrane. Moreover, AFM imaging can be performed in a partially dried state in ambient environment, whereas the conventional SEM technique used in this work requires drier samples and scanning occurs in a vacuum environment of about 10^{-3} Pa (in the chamber). Drying can also introduce changes into the surface morphology of the polymers and may alter or obscure the features of interest. Note that, for SEM a magnification of 50,000 times using 10 kV acceleration voltage was limiting for membrane samples. Higher magnification leads to strong local heating of the sample by the electron beam and subsequent melting of the membrane area under investigation. Therefore, low-voltage operation in the specimen chamber sacrifices resolution. In addition, unlike SEM, the AFM can measure in all three dimensions (x, y, and z) including height information with a vertical resolution of <1 nm. The three-dimensional nature of the AFM can be used to estimate changes in roughness and surface area variations. At the same time, SEM has the ability to image very rough samples due to its large depth of field and large lateral field of view. And we used this advantage of SEM to visualize the microrelief of rough PAni layer for surface modified composites, which will be discussed later.

3D images of the membrane surface topography (scan size 5 μm × 5 μm) obtained by the AFM method are presented in Fig. 4. Fig. 4a shows that unmodified membrane has a relatively flat surface. After modification, a change in surface topography is observed. It can be seen from Fig. 4b that after 5 h of synthesis PAni forms on the surface particles of no more than 20–30 nm in height and 40–100 nm in diameter. PAni microdomens in the form of granules or hemispheres with a diameter of 200 nm up to 1.4 μm and a height of up to 300 nm are characteristic of the membrane PAni/MF-4SC surface after 30 days of synthesis (Fig. 4c). The "germination"

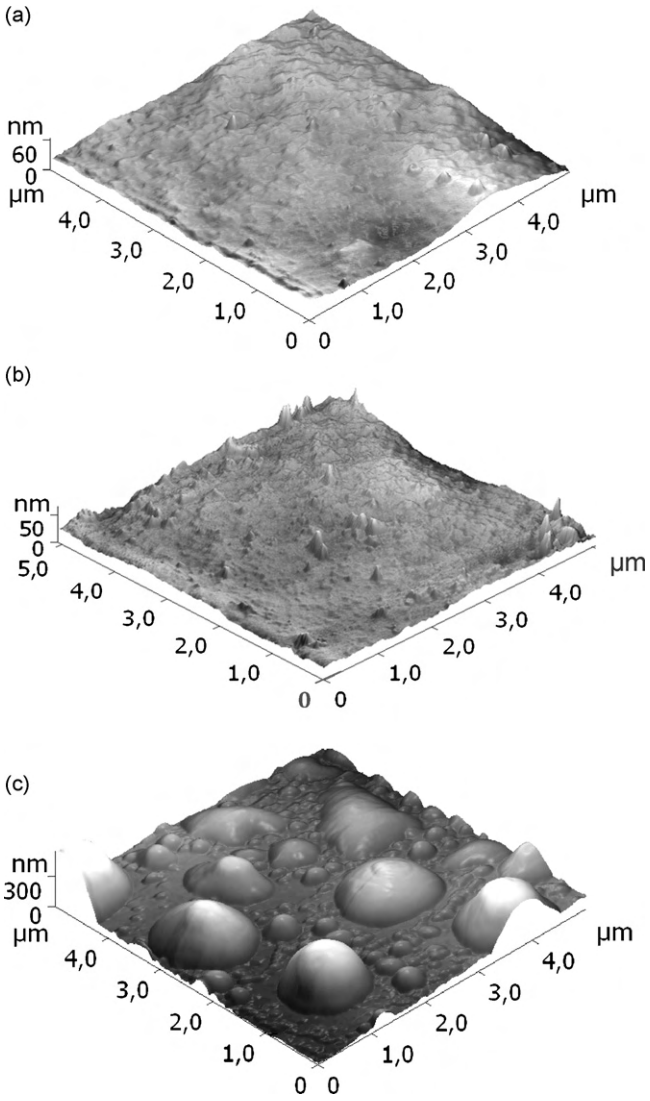

Fig. 4. AFM images of MF-4SC (a), PAni/MF-4SC after 5 h (b) and 30 days (c) of synthesis.

of PAni to the membrane surface is also observed during the electrochemical synthesis of polyaniline, where its formation owing to electrons from the electrode surface occurs [27]. The change of the surface topography in Fig. 4 demonstrates the transition of PAni from a nanosized to a microsized morphology; as a consequence, transport properties of the samples under investigation change.

The change in the inhomogeneity degree of the composite membranes is confirmed by the data on standard porosimetry. Water distribution (v, cm^3/g) inside the composite membrane samples is shown in Fig. 5. Fig. 5a shows that, if the polymerization time of aniline in the base matrix does not exceed 10 h, there is no essential change in the porosimetry curves, which indirectly confirms the formation of nanosized inclusions of PAni inside the membrane. After 5–10 h of polymerization (emeraldine form and green color) the effective pore radius is not bigger than 80 nm. The porosimetry method has shown earlier [38,39] that the effective pore radius of structural cavities in the swollen perfluorinated membranes, Nafion and MF-4SC, is equal to 100–200 nm. Pores of this radius disappear when the implantation of PAni chains occurs. This confirms the nanosized character of PAni inclusions.

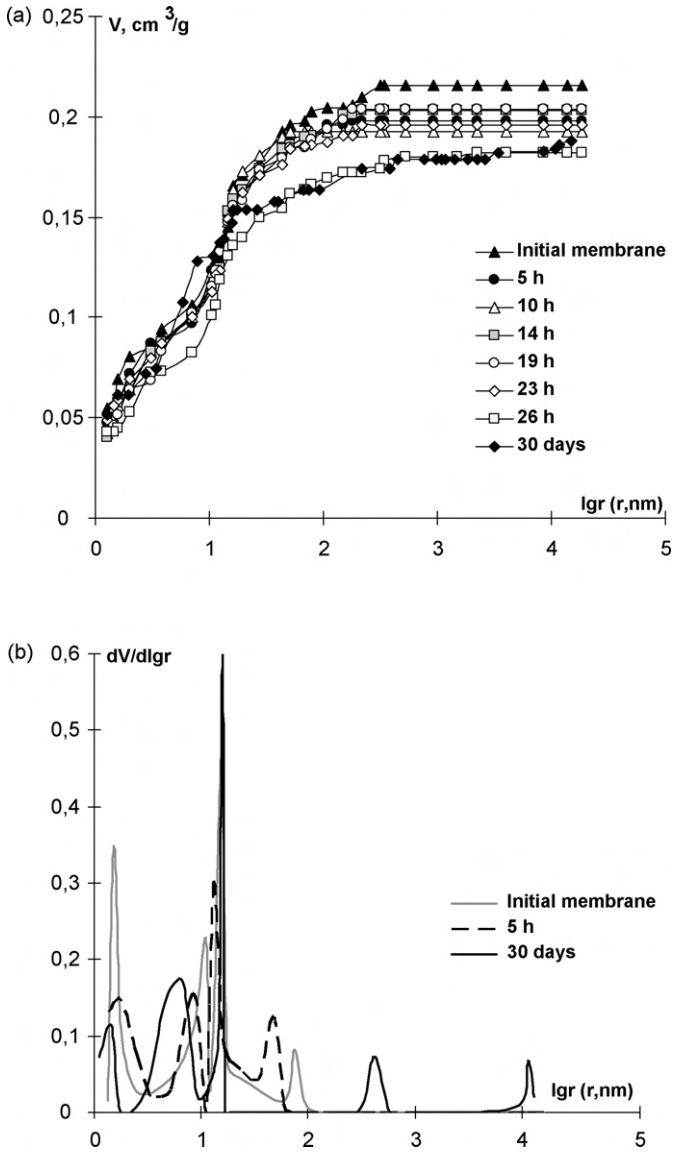

Fig. 5. Integral (a) and differential (b) functions of water distribution on the effective pore radii for a MF-4SC membrane and composites after various times of aniline polymerization.

Changes in structural characteristics of the composite membranes are observed after 26 h and become very significant after 30 days of synthesis. Fig. 5a also shows that the maximum value of water content decreases by 8–15% as the polymerization time of aniline increases. This is in agreement with the data of independent gravimetric measurements of water uptake (Table 1) and data of paper [79].

It can be seen from the differential porosimetry curves (Fig. 5b) that after 26 h of polymerization of aniline, where emeraldine transforms to pernigraniline, the formation of structural cavities with a pore radius of 300 nm is detected. For a membrane sample, where PAni was synthesized for 30 days, a small peak at about 10 μm pore radius is observed, which corresponds to a water bonding energy of 1 J/mol or below. This weakly bonded water is removed from the membrane during its drying first because, most likely, this water is localized in defects on the membrane surface. The increase of the volume of large pores in the composite after 30 days of synthesis is in agreement with the increase of structural parameter f_2 of the model (Table 2).

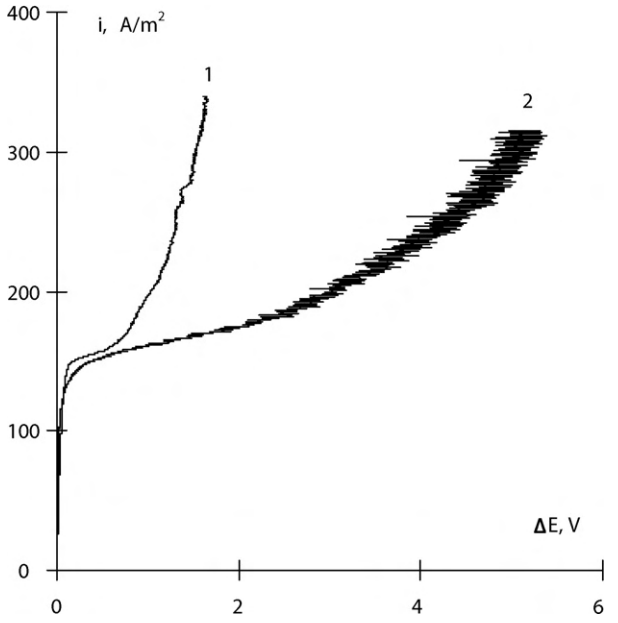

Fig. 6. Current–voltage curves of a MF-4SC membrane (1) and composite PAni/MF-4SC after 5 h of synthesis (2) measured in a 0.025 M H_2SO_4 solution.

3.3. Polarization characteristics of composite membranes

3.3.1. Current–voltage curves of composite membranes

In order to investigate the polarization behavior of the composites PAni/MF-4SC, their current–voltage curves were recorded. As one can see from Fig. 6 and Table 4, the slopes of the ohmic part of CVCs for the original membrane and for the composite one after 5 h of synthesis are the same. It is in agreement with the results on the conductivity of these composites measured under alternating current [29,30]. The values of the limiting current density are also practically the same for the two membranes, which agrees with their TSP values [80]. The close values of i_{lim} before and after modification (Fig. 6) can be explained by mutual compensation of two opposite factors: increase of i_{lim} due to solution electroconvection (which, in turn, is due to the surface microrelief growth) and decrease of i_{lim} due to the growth of the surface area.

The effect of a longer plateau of the limiting current was observed in the CVC of the PAni/MF-4SC composites (curve 2). The potential of transition to the overlimiting state for the composite membranes is above 3 V, whereas for the original membrane this value is $\Delta E_{cr} \approx 0.85$ V. Such an effect was observed for composites based on both industrial and pilot samples of the MF-4SC membrane [80]. It has been shown that the plateau length depends on the nature and concentration of solution, characteristics of the original membrane and PAni oxidation degree. We assumed that the water energy state in the composite membrane is a key factor determining the potential of transition to the overlimiting state. Our assumption is confirmed by recording CVCs with simultaneous registration of the pH value of solution in membrane vicinity [80].

Table 4
Parameters of the current–voltage curves of different membranes in a 0.025 M H_2SO_4 solution.

Membrane	i_{lim} (A/m^2)	ΔE_{lim} (V)	ΔE_{cr} (V)	Δ (V)
MF-4SC	145 ± 9	0.039 ± 0.011	0.84 ± 0.10	0.80 ± 0.09
PAni/MF-4SC (5 h of synthesis)	147 ± 1	0.032 ± 0.001	3.29 ± 0.18	3.25 ± 0.18

3.3.2. Asymmetry of current–voltage curves of anisotropic composites

It was of interest to investigate CVCs of composites containing PAni in the surface layer. Such composites were synthesized according to the method proposed in work [79] for Nafion-based composites. In this case, the original membrane being saturated with aniline is placed between two compartments of the cell with a 0.1 M $(NH_4)_2S_2O_8$ solution (polymerization initiator) and water respectively. Polyaniline was obtained by the diffusion of the $(NH_4)_2S_2O_8$ solution through the membrane for 2 h.

The SEM images shown in Fig. 7 may be an indication of the composite anisotropy. Images of the original "bare" MF-4SC membrane surface, of the composite membrane surface being in contact with the initiator solution during synthesis and of the surface being in contact with water are shown in Fig. 7a–c respectively. These images were taken with a magnification of 30,000 up to 50,000 times in the secondary electron mode, i.e. bright and dark areas in the image are characteristic of the sample topography. The PAni coating (Fig. 7b) seems to be friable; displaying some aggregates along with some structural cavities. But obviously, a portion of PAni chains could grow through the membrane to the other side since the

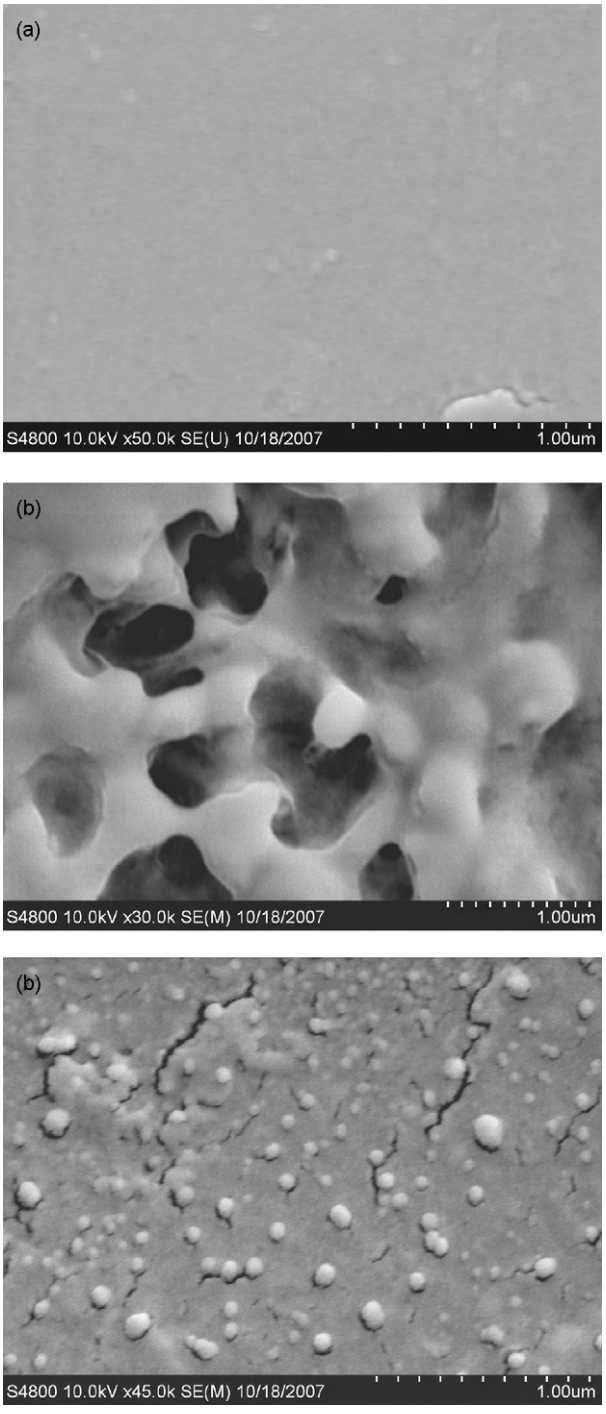

Fig. 7. SEM images of a MF-4SC membrane (a) and of an anisotropic composite PAni/MF-4SC (b, c): (b) is the side with PAni layer on it and (c) is the opposite side.

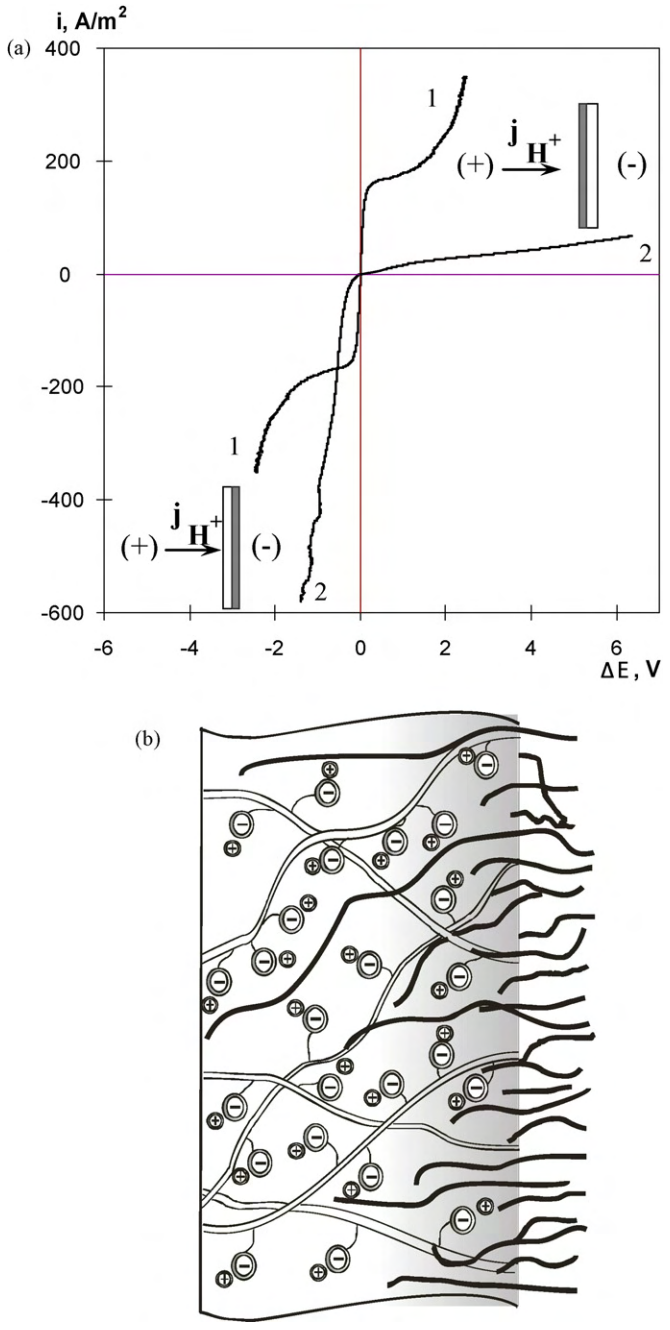

Fig. 8. (a) Current–voltage curves of a MF-4SC membrane (1) and of an anisotropic composite PAni/MF-4SC (2) in a 0.05 M HCl solution; curves in the top right section correspond to position I of the membrane, while curves in the bottom left section correspond to position II of the membrane; (b) schematic presentation of a perfluorinated membrane MF-4SC after surface modification by polyaniline.

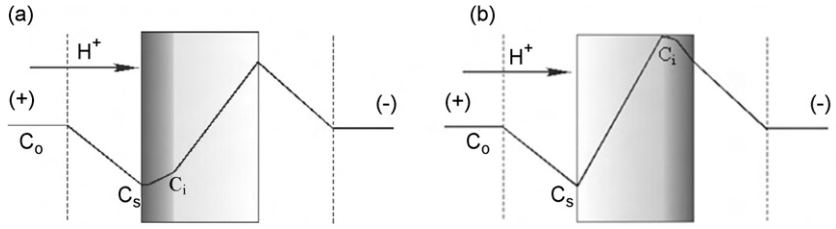

Fig. 9. Concentration profiles formed under currents below limiting for PAni/MF-4SC composite membranes being in position I (a) and position II (b) C_0 – concentration of H^+ ions in the external solution; C_s – concentration of H^+ ions on the membrane surface; C_i – concentration of H^+ ions at the internal membrane/modified layer interface.

diffusion transport of polymerization solutions occurs. As a result, we can observe PAni grains (40–100 nm in diameter) on the side of the composite membrane being in contact with water (Fig. 7c). Also, this image shows some cracks on the surface of the gold layer covering the membrane, which appear during image acquisition. These cracks formed most likely due to water removal from the membrane and burning effects. It should also be noted that SEM probes a few micrometers deep and the image acquired is actually an image of the first few micrometers of the sample. And we can conclude that PAni grain-like structure is possibly present both on the surface of the membrane and in its bulk [68].

The presence of PAni on both sides of the composite membrane is confirmed by the data of elemental analysis. The EDS quantitative in-depth microanalysis was effective in measuring approximate concentration ratios of the elements in 50–100 μm width areas of membranes before and after surface modification by PAni. The volume which is penetrated by the multiply scattered primary electrons and exited to produce X-ray radiation reaches 5 μm in depth. It was shown that in the original membranes main elements of a perfluorinated sulfoacid appear. An essential decrease of fluorine content was observed for all composite membrane samples. It confirms the presence of another component in membrane, which does not contain fluorine. The characteristic X-ray intensities of nitrogen were detected on both sides of surface modified membrane.

The anisotropic structure of these membranes was confirmed by independent measurements of their diffusion permeability in HCl solutions. The coefficient of asymmetry of diffusion permeability A_p for different orientations of the composite membrane towards the acid flux was calculated:

$$A_p = \frac{p_s}{p_w} \tag{15}$$

where P_s is the integral coefficient of diffusion permeability of membrane in position I (PAni layer towards the acid solution), P_w is the integral coefficient of diffusion permeability of membrane in position II (PAni layer towards water). The value of A_p is 0.78.

Effects of transport properties asymmetry for the modified membranes with anisotropic structure including polarization characteristics were studied in a number of works [81–84]. For the composites obtained in this work CVCs were measured in a 0.05 M HCl solution (Fig. 8a). When the composite membrane is in position I a drastic increase of the resistance (by 2 orders of magnitude) and decrease of the limiting current are observed in comparison with the initial membrane. In contrast to bulk-modified membranes, a limiting current plateau is practically not observed in the case of anisotropic composites. A polyaniline layer imparts electrical heterogeneity to the membrane surface, which is due to the development of a microrelief (Fig. 8b). The presence of a microrelief may also result in the appearance of laminar microflows, which change the thickness of the diffusion layer. As a result, the limiting state does not set in simultaneously on the whole membrane surface, which is displayed by coupled effects of concentration polarization. Thus the area of a CVC after the ohmic part corresponds to a "pseudo-limiting" state of the system.

When the composite membrane is in position II, the CVC changes essentially. The total resistance of the system in the ohmic part of a CVC in this case is more than 10 times as low as for the initial membrane. It allows to conclude about asymmetry of conducting properties of the composite membrane. The sharp growth of the current in a CVC (instead of the appearance of a limiting current plateau) does not allow to register the onset of the limiting state. This effect is related to the presence of polyaniline both on the surface and in the bulk of the membrane.

We can explain the decrease of PAni/MF-4SC composite resistance in position II based on the analysis of concentration profiles formed in the course of polarization (Fig. 9). It is known that under polarization of an electromembrane system the concentration of H^+ ions at the external membrane/solution interface decreases, whereas inside the membrane it increases. Under these conditions, the accumulation of H^+ ions at the internal membrane/modified layer interface may occur. Therefore an increase in the slope of the ohmic part is observed in the CVC. This phenomenon could be related to the doping of polyaniline macromolecules by the protons accumulated and configurational changes of the former [67]. However, changes in water energy state are not excluded, which might take place in anisotropic composites as well. But this question requires additional research.

4. Conclusions

Transport properties of PAni/MF-4SC composite membranes (after bulk modification) – conductivity, diffusion and electroosmotic permeability, proton permselectivity – as well as porosimetry and polarization behavior have been investigated as functions of aniline polymerization parameters and acid concentration. The fibrous-cluster model of a composite membrane has been proposed for the estimation of transport and structural parameters, taking into consideration different mechanism of charge transfer in structural fragments of the composite. The atomic force microscopy images and curves of water distribution on the effective pore radii in the composite membranes testify to a morphological transition from the nano- to the microsize of polyaniline intercalations with increasing the aniline polymerization time. This effect is confirmed by the analysis of two-phase model transport and structural parameters. High values of the "true" proton transport numbers of composites have been obtained and discussed. The dynamic hydration numbers of protons and chloride co-ions have been estimated using the "true" transport numbers of protons and the electroosmotic coefficients of composites.

The current–voltage curves of composite membranes in the "free standing" state after both bulk and surface modification by polyaniline have been investigated in acid solutions. New polarization effects depending on the oxidation degree of polyaniline and morphology of the composite membrane have been

discovered. The effect of stabilization of limiting current density is observed for MF-4SC membrane after bulk modification. The effect of current–voltage curves asymmetry is observed for different orientation of the polyaniline layer towards the current direction for an anisotropic composite membrane after surface modification.

It has been shown that polyaniline intercalations allow to optimize the structure and properties of composite membranes.

Acknowledgements

The authors are thankful to Dr. S.V. Timofeev (Plastpolymer, Saint-Petersburg) for the samples of MF-4SC membranes and to Dr. J. Sytchev (Institute for Nanotechnology, Miskolc) for his valuable help in editing this paper. The financial support by the Russian Foundation for Basic Research (project RFBR 08-08-00609) is gratefully acknowledged.

References

[1] M.R. Tarasevich, S.B. Orlov, E.I. Shkolnikov, et al. (Eds.), Electrochemistry of Polymers, Nauka, Moscow, 1990 (in Russian).
[2] H. Strathmann, in: H. Strathmann (Ed.), Membrane Science and Technology, vol. 9, Elsevier, 2004 (preface).
[3] T. Sata, Ion-exchange Membranes, Royal Society of Chemistry, Cambridge, 2004.
[4] A. Pud, N. Ogurtsov, A. Korzhenko, G. Shapoval, Prog. Polym. Sci. 28 (2003) 1701.
[5] M.A. Vorotyntsev, S.V. Vasilyeva, Adv. Colloid Interface Sci. 139 (2008) 97.
[6] J. Roeder, V. Zucolotto, S. Shishatskiy, J.R. Bertolino, S.P. Nunes, A.T.N. Pires, J. Membr. Sci. 279 (2006) 70.
[7] A. Montes Rojas, Y. Olivares Maldonado, L.M. Torres Rodriguez, J. Membr. Sci. 300 (2007) 2.
[8] F.D.R. Amado, M.A.S. Rodrigues, F.D.P. Morisso, A.M. Bernardes, J.Z. Ferreira, C.A. Ferreira, J. Colloid Interface Sci. 320 (2008) 52.
[9] A.A. Nekrasov, O.L. Gribkova, T.V. Eremina, A.A. Isakova, V.F. Ivanov, V.A. Tverskoj, A.V. Vannikov, Electrochim. Acta 53 (2008) 3789.
[10] R.K. Nagarale, G.S. Gohil, V.K. Shahi, G.S. Trivedi, R. Rangarajan, J. Colloid Interface Sci. 277 (2004) 162.
[11] R.H. Thring (Ed.), Fuel Cells for Automotive Applications, Professional Engineering Publishing, Bury St. Edmunds and London, 2004.
[12] K.-D. Kreuer, S.J. Paddison, E. Spohr, M. Schuster, Chem. Rev. 104 (2004) 4637.
[13] S. Prakash, Ch.R.K. Rao, M. Vijayan, Electrochim. Acta 53 (2008) 5704.
[14] K.D. Kreuer, M. Schuster, B. Obliers, O. Diat, U. Traub, A. Fuchs, U. Klock, S.J. Paddison, J. Maier, J. Power Sources 178 (2008) 499.
[15] C. Heitner-Wirguin, J. Membr. Sci. 120 (1996) 1.
[16] A.F. Mazanko, G.M. Kamaryan, O.P. Romashin, Industrial Membrane Electrolysis, Khimiya, Moscow, 1989 (in Russian).
[17] V. Gupta, N. Miura, Mater. Lett. 60 (2006) 1466.
[18] T. Shimizu, T. Naruhashi, T. Momma, T. Osaka, Electrochemistry 70 (2002) 991.
[19] D. Sazou, D. Kosseoglou, Electrochim. Acta 51 (2006) 2503.
[20] C.-Y. Chen, J.I. Garnica-Rodriguez, M.C. Duke, R.F. Dalla Costa, A.L. Dicks, J.C. Diniz da Costa, J. Power Sources 166 (2007) 324.
[21] S. Tan, A. Laforgue, D. Belanger, Langmuir 19 (2003) 744.
[22] S. Tan, V. Viau, D. Cugnod, D. Belanger, Electrochem. Solid State Lett. 5 (2002) E55.
[23] P. Sivaraman, J.G. Chavan, A.P. Thakur, V.R. Hande, A.B. Samui, Electrochim. Acta 52 (2007) 5046.
[24] A. Yasuda, T. Shimidzu, Polym. J. 25 (1993) 329.
[25] G. Li, L. Jiang, H. Peng, Macromolecules 40 (2007) 7890.
[26] S. Tan, J.H. Tieu, D. Bélanger, J. Phys. Chem. B 109 (2005) 14085.
[27] N.M. Alpatova, V.N. Andreev, A.I. Danilov, E.B. Molodkina, Yu.M. Polukarov, N.P. Berezina, S.V. Timofeev, L.P. Bobrova, N.N. Belova, Rus. J. Electrochem. 38 (2002) 913.
[28] N.P. Berezina, A.A.-R. Kubaisy, N.M. Alpatova, V.N. Andreev, E.I. Griga, Rus. J. Electrochem. 40 (2004) 286.
[29] N.P. Berezina, A.A.-R. Kubaisy, Rus. J. Electrochem. 42 (2006) 81.
[30] N.P. Berezina, A.A.-R. Kubaisy, S.V. Timofeev, L.V. Karpenko, J. Solid State Electrochem. 11 (2007) 378.
[31] N.P. Berezina, S.V. Timofeev, N.A. Kononenko, J. Membr. Sci. 209 (2002) 509.
[32] S. Rowland (Ed.), Water in Polymers, Mir, Moscow, 1984 (in Russian).
[33] M. Fabrizio, G. Mengoli, M.M. Musiani, F. Paolucci, J. Electroanal. Chem. 300 (1991) 23.
[34] E.K.W. Lai, P.D. Beattie, F.P. Orfino, E. Simon, S. Holdcroft, Electrochim. Acta 44 (1999) 2559.
[35] J.-C. Chiang, A.G. Macdiarmid, Synth. Met. 13 (1986) 193.
[36] N.P. Gnusin, N.P. Berezina, O.A. Dyomina, N.A. Kononenko, Rus. J. Electrochem. 32 (1996) 154.
[37] G. Pourcelly, A. Oikonomou, C. Gavach, H.D. Hurwitz, J. Electroanal. Chem. 287 (1990) 43.
[38] Yu.M. Volfkovich, V.S. Bagotzky, V.E. Sosenkin, I.A. Blinov, Colloids Surf. A: Physicochem. Eng. Aspects 187–188 (2001) 349.
[39] J. Divisek, M. Eike, V. Mazin, H. Schmitz, U. Stimming, Yu.M. Volfkovich, J. Electrochem. Soc. 45 (1998) 2677.
[40] N.P. Berezina, Yu.M. Volfkovich, N.A. Kononenko, I.A. Blinov, Rus. J. Electrochem. 23 (1987) 858.
[41] N.P. Berezina, N.A. Kononenko, Yu.M. Volfkovich, Rus. J. Electrochem. 30 (1994) 329.
[42] N.P. Berezina, N.A. Kononenko, O.A. Dyomina, N.P. Gnusin, Adv. Colloid Interface Sci. 139 (2008) 3.
[43] G.B. Binnig, C.F. Quate, Ch. Gerber, Phys. Rev. Lett. 12 (1986) 930.
[44] V.L. Mironov, Fundamentals of Scanning Probe Microscopy, Nizhniy Novgorod, The Russian Academy of Science, Institute of Physics of Microstructures, 2004.
[45] A. Lehmani, S. Durand-Vidal, P. Turq, J. Appl. Polym. Sci. 68 (1998) 503.
[46] N.P. Berezina, S.V. Timofeyev, A.-L. Rollet, N.V. Fedorovich, S. Durand-Vidal, Rus. J. Electrochem. 38 (2002) 903.
[47] J.I. Goldstein, D.E. Newbury, P. Echlin, D.C. Joy, C. Fiori, E. Lifshin, Scanning Electron Microscopy and X-ray Microanalysis, Plenum Publishing Corp., New York, 1981.
[48] R. Nessler, Scanning 21 (1999) 137.
[49] L.V. Karpenko, O.A. Dyomina, G.A. Dvorkina, S.B. Parshikov, C. Larchet, B. Auclair, N.P. Berezina, Rus. J. Electrochem. 37 (2001) 287.
[50] V. Zabolotsky, V. Nikonenko, J. Membr. Sci. 79 (1993) 181.
[51] V.I. Zabolotsky, V.V. Nikonenko, Transport of Ions in Membranes, Moscow, 1996 (in Russian).
[52] N.P. Berezina, N.A. Kononenko, O.A. Demina, N.P. Gnusin, Polym. Sci.: Ser. A 46 (2004) 672.
[53] N.P. Gnusin, N.P. Berezina, N.A. Kononenko, O.A. Demina, J. Membr. Sci. 243 (2004) 301.
[54] N.P. Gnusin, O.A. Demina, N.P. Berezina, N.A. Kononenko, Theor. Foundat. Chem. Eng. 38 (2004) 394.
[55] N. Berezina, N. Gnusin, O. Dyomina, S. Timofeyev, J. Membr. Sci. 86 (1994) 207.
[56] N.P. Berezina, E.N. Komkova, Colloid J. 65 (2003) 1.
[57] N.P. Gnusin, N.A. Kononenko, S.B. Parshikov, Rus. J. Electrochem. 30 (1994) 28.
[58] I. Rubinstein, B. Zaltzman, Phys. Rev. E 62 (2000) 2238.
[59] J.J. Krol, M. Wessling, H. Strathmann, J. Membr. Sci. 162 (1999) 145.
[60] V.A. Shaposhnik, V.I. Vasil'eva, O.V. Grigorchuk, Transfer Phenomena in Ion-exchange Membranes, Moscow, 2001 (in Russian).
[61] V.I. Zabolotsky, V.V. Nikonenko, N.D. Pismenskaya, E.V. Laktionov, M.Kh. Urtenov, H. Strathmann, M. Wessling, G.H. Koops, Sep. Purif. Technol. 14 (1998) 255.
[62] V.V. Nikonenko, N.D. Pismenskaya, E.I. Volodina, Rus. J. Electrochem. 41 (2005) 1205.
[63] H.-J. Lee, H. Strathmann, S.-H. Moon, Desalination 190 (2006) 43.
[64] N.V. Loza, N.A. Kononenko, S.A. Shkirskaya, N.P. Berezina, Rus. J. Electrochem. 42 (2006) 815.
[65] A.B. Yaroslavtsev, V.V. Nikonenko, V.I. Zabolotsky, Rus. Chem. Rev. 72 (2003) 393.
[66] V.F. Ivanov, K.V. Cheberjako, A.A. Nekrasov, A.V. Vannikov, Synth. Met. 119 (2001) 375.
[67] V.F. Ivanov, O.L. Gribkova, S.V. Novikov, A.A. Nekrasov, A.A. Isaakova, A.V. Vannikov, G.B. Meshkov, I.V. Yaminskiy, Synth. Met. 152 (2005) 152.
[68] N.P. Berezina, A.A.-R. Kubaisy, I.A. Stenina, R.V. Smolka, S.V. Timofeev, Membr. Ser.: Crit. Technol. 32 (2006) 48 (in Russian).
[69] I.P. Suzdalev, Nanotechnology: Physic-chemistry of Nanoclusters, Nanostructures and Nanomaterials, KomKniga, Moscow, 2006 (in Russian).
[70] C. Larchet, B. Auclair, V. Nikonenko, Electrochim. Acta 49 (2004) 1711.
[71] N.P. Gnusin, N.A. Kononenko, S.B. Parshikov, Rus. J. Electrochem. 29 (1993) 647.
[72] N.P. Gnusin, S.B. Parshikov, O.A. Dyomina, Rus. J. Electrochem. 34 (1998) 1185.
[73] J. Vargas, A.A. Santiago, M.A. Tlenkopatchev, R. Gavino, M.F. Laguna, M. Lopez-Gonzalez, E. Riande, Macromolecules 40 (2007) 563.
[74] V. Compañ, E. Riande, F.J. Fernandez-Carretero, N.P. Berezina, A.A.-R. Sytcheva, J. Membr. Sci. 318 (2008) 255.
[75] N.P. Berezina, S.A. Shkirskaya, A.A.-R. Sytcheva, M.V. Krishtopa, Colloid J. 70 (2008) 397.
[76] J.O'M. Bockris, A.K.N. Reddy, Ionics, vol. 1, 2nd ed., New York and Plenum Press, London, 1999 (Chapter 4).
[77] R.A. Robinson, R.H. Stokes, Electrolyte Solutions, Academic Press Ltd., London, 1959.
[78] K.D. Kreuer, J. Membr. Sci. 185 (2001) 29.
[79] S. Tan, D. Bélanger, J. Phys. Chem. 109 (2005) 23480.
[80] N.P. Berezina, N.A. Kononenko, N.V. Loza, A.A.-R. Sycheva, Rus. J. Electrochem. 43 (2007) 1340.
[81] A.N. Filippov, V.M. Starov, N.A. Kononenko, N.P. Berezina, Adv. Colloid Interface Sci. 139 (2008) 29.
[82] R. Ibanez, D.F. Stamatialis, M. Wessling, J. Membr. Sci. 239 (2004) 119.
[83] G. Chamoulaud, D. Bélanger, J. Colloid Interface Sci. 281 (2005) 179.
[84] I. Rubinstein, B. Zaltzman, in: T.S. Sorensen (Ed.), Surface Chemistry and Electrochemistry of Membranes, vol. 79, Dekker, New York, 1999 (Chapter 3).